Neurochem Res (2016) 41:2490–2500
DOI 10.1007/s11064-016-1981-2

ORIGINAL PAPER

SIRT2 Plays Significant Roles in Lipopolysaccharides-Induced Neuroinflammation and Brain Injury in Mice

Ban Wang[1] · Youjun Zhang[3] · Wei Cao[1] · Xunbing Wei[1] · James Chen[4] · Weihai Ying[1,2]

Received: 14 January 2016 / Revised: 18 April 2016 / Accepted: 22 April 2016 / Published online: 27 June 2016

Abstract Several recent studies have suggested seemingly contrasting roles of SIRT2 in inflammation: Our previous cell culture study has indicated that SIRT2 siRNA-produced decrease in SIRT2 levels can lead to significant inhibition of lipopolysaccharides (LPS)-induced activation of BV2 microglia, suggesting that SIRT2 is required for LPS-induced microglial activation. In contrast, some studies have suggested that SIRT2 deficiency can lead to increased inflammation. In our current study, we used a mouse model of neuroinflammation to determine the roles of SIRT2 in LPS-induced inflammation. We found that administration of SIRT2 inhibitor AGK2 can significantly decrease LPS-induced increases in CD11b signals and the mRNA of TNF-α and IL-6. We further found that AGK2 can block LPS-induced nuclear translocation of NFκB. In addition, our study has shown that AGK2 can decrease not only LPS-induced increase in TUNEL signals—a marker of apoptosis-like damage, but also LPS-induced increases in the levels of active Caspase-3 and Bax. Collectively, our current in vivo study, together with our previous cell culture study, has suggested that SIRT2 is required for LPS-induced neuroinflammation and brain injury.

Keywords SIRT2 · Neuroinflammation · Brain · Cytokines · Apoptosis

Introduction

Sirtuins are NAD^+-dependent histone deacetylase that play important roles in various biological functions [1–7]. SIRT2 inhibition or deficiency has been shown to produce neuroprotective effects in models of both neurodegenerative diseases [8] and ischemia stroke [9]: SIRT2 inhibition led to a decrease in 1-methyl-4-phenyl-1,2,3,6-tetrahydropyridine (MPTP)-induced nigrostriatal damage [10]; SIRT2 deletion was shown to decrease α-synuclein-induced neurotoxicity in models of Parkinson's disease [11]; SIRT2 inhibitor AK-7 was shown to produce beneficial effects in a mouse model of HD [12]; and SIRT2 deficiency mice also showed decreased neurological deficits after ischemia stroke [9]. However, it is warranted to investigate the mechanisms underlying the neuroprotective effects of SIRT2 inhibition.

Because multiple studies have suggested a critical pathological role of inflammation in ischemia stroke [13] and certain neurodegenerative diseases [14, 15], we hypothesized that the beneficial effects of SIRT2 inhibition in the disease models may result from its capacity to inhibit inflammation. Our previous cell culture study has indicated that SIRT2 siRNA-produced decrease in SIRT2 levels can lead to significant inhibition of lipopolysaccharides (LPS)-induced activation of BV2 microglia, suggesting that SIRT2

Electronic supplementary material The online version of this article (doi:10.1007/s11064-016-1981-2) contains supplementary material, which is available to authorized users.

✉ Weihai Ying
weihaiy@sjtu.edu.cn

1 Med-X Research Institute and School of Biomedical Engineering, Shanghai Jiao Tong University, 1954 Huashan Road, Shanghai 200030, People's Republic of China

2 Department of Neurology, Ruijin Hospital, Shanghai Jiao Tong University School of Medicine, Shanghai 201999, People's Republic of China

3 Cardiology Department, Shanghai Chest Hospital, Shanghai Jiao Tong University, Shanghai 200030, People's Republic of China

4 Department of Biomedical Engineering, Johns Hopkins University, Baltimore, MD, USA

Springer

is required for LPS-induced microglial activation [16]. In contrast, there have been other studies suggesting that SIRT2 inhibition can lead to increased inflammation [17, 18]. Therefore, it is warranted to further investigate the roles in SIRT2 in inflammation.

By using LPS-induced neuroinflammation of mice as an in vivo model, in the current study we determined the roles of SIRT2 in inflammation. Our study has suggested that SIRT2 is required for LPS-induced neuroinflammation and brain injury in vivo.

Materials and Methods

Reagents

All of the chemicals were purchased from Sigma (St. Louis, Missouri, USA), except where specified.

Ethics Statement

This study was carried out in strict accordance with the recommendations in the Guide for the Care and Use of Laboratory Animals of the Shanghai Administrative Committee. All of the animal protocols were approved by the Animal Study Committee of the School of Biomedical Engineering, Shanghai Jiao Tong University (Permit Number: 2011001). All surgical procedures were performed by Ban Wang (Qualification Certificate Number: 14080366) under chloral hydrate anesthesia, in which all efforts were made to minimize animal suffering. Mice were sacrificed by cervical dislocation at designed time points as shown in Results.

Procedures of Animal Operation

A total of 149 adult male C57BL/6 mice (107 mice for frozen section, 18 mice for real-time PCR and 24 mice for Western blot assay) weighing 22–25 g were purchased from SLRC Laboratory (Shanghai, China). Considering the tissue toxicity of DMSO [19] and the limit of the volume of the solution injected into the mouse brain, in our study we administered two dosages of AGK2, 0.5 μmol/mouse and 1 μmol/mouse. AGK2 was dissolved in DMSO and diluted in PBS. The final concentrations of AGK2 for the two dosages of AGK2 were 100 and 200 μM, with 4 % final concentration of DMSO. Mice were randomly divided into 6 groups: (a) The Vehicle group (PBS containing 4 % DMSO); (b) SIRT2 inhibitor (0.5 μmol AGK2 per mouse) group; (c) SIRT2 inhibitor (1 μmol AGK2 per mouse) group; (d) LPS treatment (4 μg LPS per mouse) group; (e) LPS (4 μg LPS per mouse) and SIRT2 inhibitor (0.5 μmol AGK2 per mouse) co-administration group; (f) LPS (4 μg per mouse) and SIRT2 inhibitor (1 μmol AGK2 per mouse) co-administration group. The animals were anesthetized with chloral hydrate intraperitoneally and positioned in a small animal stereotaxic apparatus (RWD lifescience, Shenzhen, Guangdong, China). A small skull hole was made using a microsurgical drill followed by a Hamilton syringe (Hamilton, Bonaduz, Switzerland) injection (5 μL per mouse). The drug administration procedure was controlled by a MicroSyringe Pump Controller (WPI INC, Sarasota, FL, USA) and 10 min after the drug administration, the syringe was pulled out. All drugs were injected intraventricularly using the flowing stereotaxic coordinates, measured from bregma: 0.5 mm posterior, 1.1 mm lateral, and 2.6 mm ventral. No animal was dead during the experiments. Animals were sacrificed 24 h or 5 days after the drug administration. The brains were immediately removed and frozen in pre-chilled isopentane, and then stored at −80 °C until further analysis.

Immunofluorescence Assay

Brain cryosections (20 μm) were fixed in 4 % paraformaldehyde for 15 min, followed by three washes with PBS. The sections were incubated in 10 % goat serum for 1 h at room temperature and then incubated with rat monoclonal CD11b antibody (1:100 dilution, BD Biosciences, San Diego, CA, USA) in PBS containing 1 % goat serum overnight at 4 °C. After three washes with PBS, the sections were incubated with Alexa Fluor® 488 goat anti-rat IgG (H + L) Secondary antibody (1:500 dilution, Molecular Probes, Eugene, Oregon, USA) in PBS containing 1 % goat serum for 1 h at room temperature. After three washes with PBS, the sections were counterstained with DAPI (1:1000 dilution, Beyotime Institute of Biotechnology, Shanghai, China) in PBS for 5 min at room temperature. The fluorescence images of the slices were photographed under a Leica confocal fluorescence microscope (Leica TCS SP5 II, Heidelberg, Germany). Negative controls were incubated with PBS containing 1 % goat serum instead of primary antibody.

Real-Time PCR

The real-time PCR assays were conducted as described previously [20, 21]: TaKaRa MiniBEST Universal RNA Extraction Kit (Takara Bio, Dalian, China) was used to isolate total RNA from the whole brain. A Prime-Script RT reagent kit (Takara Bio) was used to reverse-transcribe 1 μg total RNA to cDNA. The RT-PCR reactions were performed under the following conditions: 37 °C for 15 min, and then 85 °C for 15 s. Quantitative real-time PCR assays were performed by using SYBR Premix Ex Taq (Takara Bio) as well as the following primers: IL-6 (sense 5′-TAGTCCTTCCTACCCCAATTTCC-3′ and

anti-sense 5′-TTGGTCCTTAGCCACTCCTTC-3′); TNF-α (sense 5′-CCCTCACACTCAGATCAT CTTCT-3′ and anti-sense 5′-GCTACGACGTGGGCTACAG-3′); GAPDH (sense 5′-AGGTCGGTGTGAACGGATTTG-3′ and anti-sense 5′-TGTAGACCATGTAGTTGAGGTCA-3′). PCR reactions were conducted under the following conditions: After denaturing at 95 °C for 10 s, 40 cycles of 95 °C for 5 s and 60 °C for 30 s were conducted. The comparative threshold cycle method was used to analyze the data, and the results were expressed as fold difference normalized to the level of GAPDH mRNA.

Immunohistochemistry Staining

Briefly, brain cryosections (20 μm) were fixed in 4 % paraformaldehyde for 15 min, followed by three washes of PBS. The sections were treated with 3 % hydrogen peroxide in methanol for 10 min and then incubated in blocking solution (10 % goat serum and 3.5 ‰ Triton X-100 in PBS) for 1 h at room temperature. The slides were incubated with primary antibody (rabbit monoclonal cleaved Caspase-3 antibody, 1:300 dilution, Cell Signaling Technology, Danvers, MA, USA; rabbit monoclonal NFκB p65 antibody, 1:300 dilution, Abcam, Cambridge, UK) in PBS containing 1 % goat serum overnight at 4 °C. After three washes with PBS, the sections were incubated with biotinylated anti-rabbit IgG antibody (1:200 dilution, Vector Laboratories Inc., Burlingame, California, USA) in PBS containing 1 % goat serum for 30 min at room temperature. After three washes with PBS, the sections were incubated with Vectastain ABC Reagent (Vector Laboratories Inc.) for 30 min at room temperature. Following three washes with PBS, the sections were incubated with peroxidase substrate solution (Vector Laboratories Inc.) for 3–5 min at room temperature. Following three washes with tap water, the sections were incubated with Hematoxylin Staining Solution (Beyotime Institute of Biotechnology) for about 1 min and washed three times with distilled water. Subsequently the sections were dehydrated in an ascending series of ethanols (70, 90, 100 %) and xylene. After mounting, the sections were viewed under a microscope (Leica). Negative controls were incubated with PBS containing 1 % goat serum instead of primary antibody.

TUNEL Staining

The TUNEL assay (Millipore, Billerica, MA, USA) was used to assess apoptosis-like DNA fragmentation in situ. We conducted the assay according to the protocol provided with the kit with minor modifications. Briefly, frozen sections (20 μm) of the brains were fixed in 1 % paraformaldehyde for 15 min, followed by three washes with PBS. The endogenous peroxidase activity of the sections was quenched by 3 % hydrogen peroxide in PBS for 5 min at room temperature. Then the sections were applied with equilibration buffer and working-strength TdT enzyme, and incubated in a humidified chamber at 37 °C for 1 h and incubated with anti-digoxigenin peroxidase for 30 min at room temperature, which was detected by DAB. Sections were counterstained in 0.5 % (w/v) methyl green for 30 min at room temperature. After the slides were washed with distilled water, the sections were dipped into 100 % *N*-butanol and xylene. After mounting, the sections were viewed under a microscope. The slices of the brains obtained 24 h after middle cerebral artery occlusion were used as positive controls. Negative control samples were prepared as other samples except that the TdT enzyme was omitted in the procedures. After mounting, the sections were viewed under a Leica microscope.

Western Blot

Western blot analysis was performed as previously described [22] with some modifications. The tissue lysates from the whole brain were harvested with Radio-Immunoprecipitation Assay (RIPA) buffer (Millipore) containing Complete Protease Inhibitor Cocktail (CWBIO, Shanghai, China) and 1 mM phenylmethanesulfonyl fluoride. The lysates were centrifuged at 14,000 g for 15 min at 4 °C. Nuclear tissue lysates from the whole brain were harvested with Nuclear and Cytoplasmic Extraction Kit (CWBIO) according to manufacturer's instructions. And then the protein concentration was quantified by the BCA assay kit (Thermo Scientific, Waltham, MA, USA). 60 μg of total protein was electrophoresed through a 12.5 % or 10 % SDS–polyacrylamide gel and then transferred to a PVDF transfer membrane (Millipore) or nitrocellulose blotting memebrane (GE Healthcare Life Sciences, Freiburg, Germany). The membranes were incubated overnight at 4 °C with primary antibodies (rabbit polyclonal Caspase-3 antibody, 1:1000 dilution, Proteintech, Chicago, IL, USA; rabbit monoclonal Bax antibody, 1:1000 dilution, Abcam; goat polyclonal actin antibody, 1:200 dilution, Santa Cruz Biotechnology, Santa Cruz, CA, USA; rabbit monoclonal NFκB p65 antibody, 1:1000 dilution, Abcam;goat polyclonal Lamin A/C antibody, 1:200 dilution, Santa Cruz Biotechnology; rabbit monoclonal β-tubulin antibody, 1:1000 dilution, Abcam) in TBST containing 1 % bovine serum albumin (BSA) and then incubated with HRP-conjugated secondary antibody (1:2000 dilution, HuaAn Biotechnology, Hangzhou, Zhejiang, China) in TBST containing 1 % BSA at room temperature for 1 h. Protein signals were detected by enhanced chemiluminescence (Thermo Scientific). The intensities of the bands was quantified by a Gel-Pro Analyzer (Media Cybernetics, Silver Spring, MD, USA).

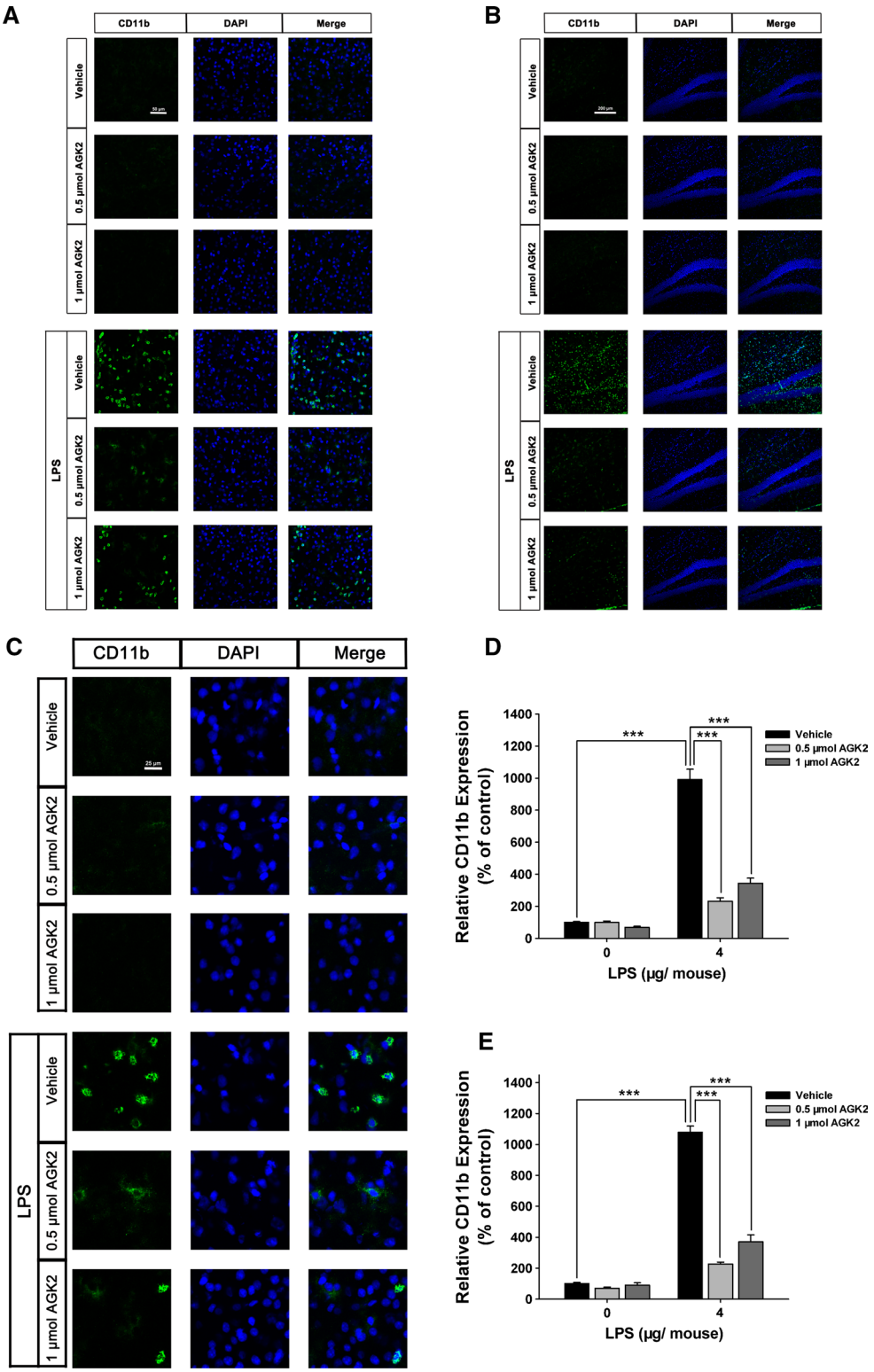

Fig. 1 SIRT2 inhibitor AGK2 suppressed the LPS-induced microglial activation in both cortex and hippocampus of the brains. **a** Representative immunofluorescence staining for CD11b (*green*) in the cortex of the brains. **b** Representative immunofluorescence staining for CD11b (*green*) in the hippocampus of the brains. Intraventricularly injected LPS (4 μg per mouse) induced a significant increase in the CD11b signals in all brain regions, including cortex and hippocampus, and simultaneous administration of AGK2 (0.5 or 1 μmol per mouse) markedly attenuated the increase 24 h after the drug administration. **c** Quantifications of the intensity of CD11b immunofluorescence in the cortex. **d** Quantifications of the intensity of CD11b immunofluorescence in the hippocampus. **e** Morphology changes of microglia in the LPS- and AGK2-treated brains. Most of the microglia in the brains of vehicle-treated mice showed ramified shape, while most of the microglia in the brains of LPS-treated mice showed ameboid shape. Administration of either 0.5 μmol AGK2/mouse or 1 μmol AGK2/mouse markedly attenuated the LPS-induced increase in the number of the microglia in ameboid shape, and markedly attenuated the LPS-induced decrease in the number of the microglia in ramified shape. Five mice for the two AGK2 treatment only groups; and Fifteen-twenty mice for the other groups. *Error bars* indicate the standard error of the mean (SEM). ***$p < 0.001$ (Color figure online)

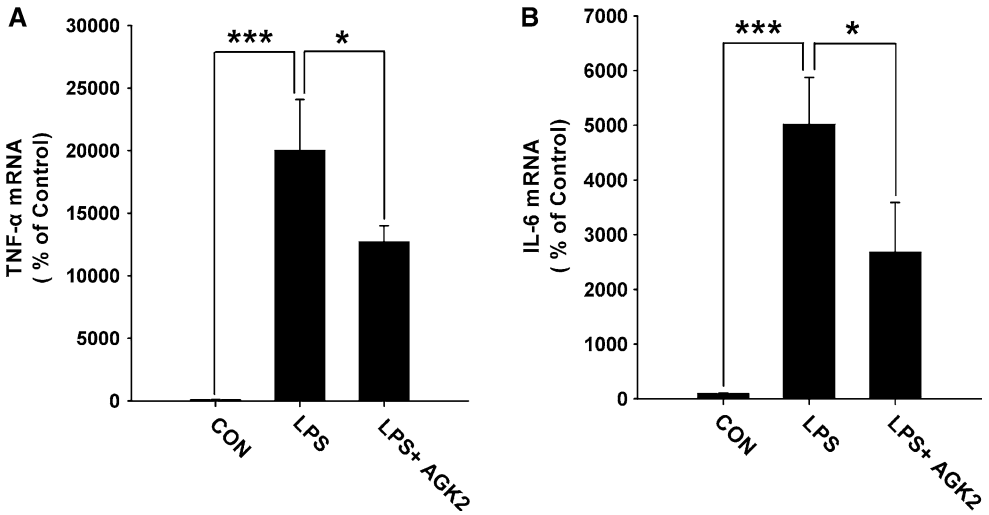

Fig. 2 SIRT2 inhibitor AGK2 inhibited the LPS-induced increases in the mRNA levels of TNF-α and IL-6 in mouse brains. AGK2 administration significantly attenuated the LPS-induced increases in the mRNA levels of TNF-α (**a**) and IL-6 (**b**) in the whole brains. The mice were intraventricularly co-injected with LPS (4 μg per mouse), with or without AGK2 (0.5 μmol per mouse) 24 h before total RNA from the whole brain was extracted. The mRNA levels of TNF-α and IL-6 were assessed by real-time PCR assays. Data were normalized by GAPDH mRNA level. Six mice in each group. *Error bars* indicate the standard error of the mean (SEM). $*p < 0.05$; $***p < 0.001$

Statistical Analyses

All data are presented as mean ± SEM. Data were analyzed by one-way ANOVA, followed by Student–Newman–Keuls post hoc test. *P* values less than 0.05 were considered statistically significant.

Results

We i.c. administered LPS into the brains, and determined the effects of LPS on the neuroinflammation in the brain. We found that LPS induced a significant increase in the CD11b signals—a marker of microglial activation [23–25] in all brain regions, including cortex (Fig. 1a, d) and hippocampus (Fig. 1b, e) of the brains. Simultaneous administration of AGK2 suppressed the LPS-induced microglial activation in all brain regions, including the cortex and hippocampus (Fig. 1). We also found that administration of the two doses of AGK2 produced similar effects on microglial activation as vehicle treatment (Fig. 1). We further determined the effects of AGK2 and LPS on the microglial activation by assessing the morphology of the microglia in the brains, since resting microglia show ramified shape, while activated microglia show ameboid shape [26–28]. We found that most of the microglia in the brains of vehicle-treated mice showed ramified shape, while most of the microglia in the brains of LPS-treated mice showed ameboid shape (Fig. 1c). Administration of both dosages of AGK2 both markedly attenuated the LPS-induced increase in the number of the microglia in ameboid shape, and markedly attenuated the LPS-induced decrease in the number of the microglia in ramified shape (Fig. 1c). To further investigate the effect of LPS and AGK2 on the brain, we determined the microglial activation 5 days after the drug administration, showing that AGK2 significantly suppressed the LPS-induced microglial activation (Supplemental Figure 1).

We also determined the effects of LPS and AGK2 on the mRNA levels of TNF-α and IL-6 in the whole brains, which are well-established markers of neuroinflammation [24, 25, 29]. We found that LPS induced significant increases in the mRNA levels of TNF-α (Fig. 2a) and IL-6 (Fig. 2b) in the brains. Simultaneous administration of AGK2 inhibited the LPS-induced increases in the mRNA levels of TNF-α and IL-6 (Fig. 2).

We further determined the effects of LPS and AGK2 on the nuclear translocation of NFκb – a key factor in neuroinflammation [30–32]—in the brains. Immunohistochemistry staining of NFκb (Fig. 3a) and Western blot of the of NFκb of the nuclear fraction (Fig. 3b, c) showed that LPS induced a significant increase in the nuclear translocation of NFκb. Simultaneous administration of AGK2 blocked the nuclear translocation of NFκb stimulated by LPS (Fig. 3).

Our study also determined the effects of AGK2 on LPS-produced brain injury. We found that LPS induced a significant increase in the TUNEL signals (Fig. 4). Simultaneous administration of AGK2 decreased LPS-induced increases in the TUNEL signals (Fig. 4). We further determined the effects of LPS and AGK2 on the active Caspase-3 level in the brains, showing that LPS induced a significant increase

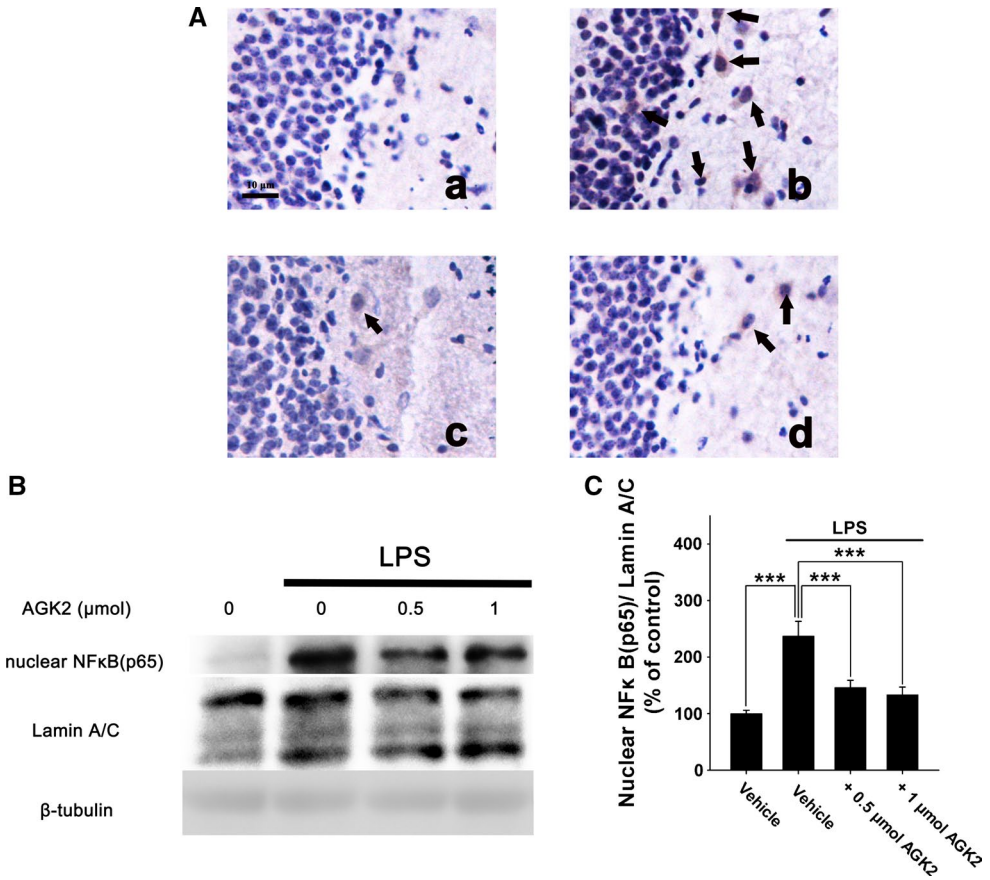

Fig. 3 SIRT2 inhibitor AGK2 attenuated the nuclear translocation of NFκb stimulated by LPS in the brains of mice. **a** Representative immunohistochemical images of NFκb in the brains of mice 24 h after the drug administration. Nuclear translocation of NFκb, indicated by arrows, was found in the LPS-injected (4 μg per mouse) mouse brains (*b*), but not in the control mouse brains (*a*). Co-administration of 0.5 μmol AGK2 (*c*) or 1 μmol AGK2 (*d*) significantly reduced the nuclear translocation of NFκb stimulated by LPS. Fifteen-twenty mice for each groups. **b** Representative Western blot of the nuclear NFκB levels in the whole brains. The mice were intraventricularly co-injected with LPS (4 μg per mouse) and AGK2 (0.5 μmol or 1 μmol per mouse) 24 h before the protein was extracted. **c** Quantifications of the protein levels of the nuclear NFκB in the mouse brains. Intraventricularly injected LPS led to a significant increase in the level of nuclear NFκB, which was blocked by co-treatment with AGK2 (0.5 or 1 μmol per mouse). Six mice in each group. *Error bars* indicate the standard error of the mean (SEM). ***$p < 0.001$ (Color figure online)

in active Caspase-3 signals, which was blocked by simultaneous administration of AGK2 (Fig. 5). Moreover, we found that LPS induced a significant increase in the protein level of Bax, which was prevented by simultaneous administration of AGK2 (Fig. 6).

Discussion

The major observations of our current study include: First, administration of SIRT2 inhibitor AGK2 can significantly suppress the LPS-induced microglial activation; second, AGK2 can significantly inhibit the LPS-induced increases in the mRNA levels of TNF-α and IL-6; third, AGK2 can prevent the translocation of NFκB stimulated by LPS from the cytosol to the nucleus; fourth, AGK2 can attenuate the LPS-induced increase in TUNEL signals—a marker of apoptosis-like damage; and fifth, AGK2 can block LPS-induced increases in the levels of active Caspase-3 and Bax. Collectively, our current in vivo study has suggested that SIRT2 is required for LPS-induced neuroinflammation and brain injury.

Multiple studies have reported that SIRT2 is expressed at high levels in both mouse and rodent brains, which is expressed in microglia [16–18, 33, 34], neurons [18, 35–38], astrocytes [18, 35, 39] and oligodendrocytes [35, 36, 39–41]. It has been reported that SIRT2 inhibition can decrease the injury in cellular and animal models of PD, HD [8] and ischemia stroke [9]. Since inflammation plays critical pathological roles in these diseases [13–15] and SIRT2 is necessary for bacteria infection [6], we hypothesized that SIRT2 may be important for neuroinflammation. The observations of our current study have suggested that decreased SIRT2 activity can lead to a significant decrease

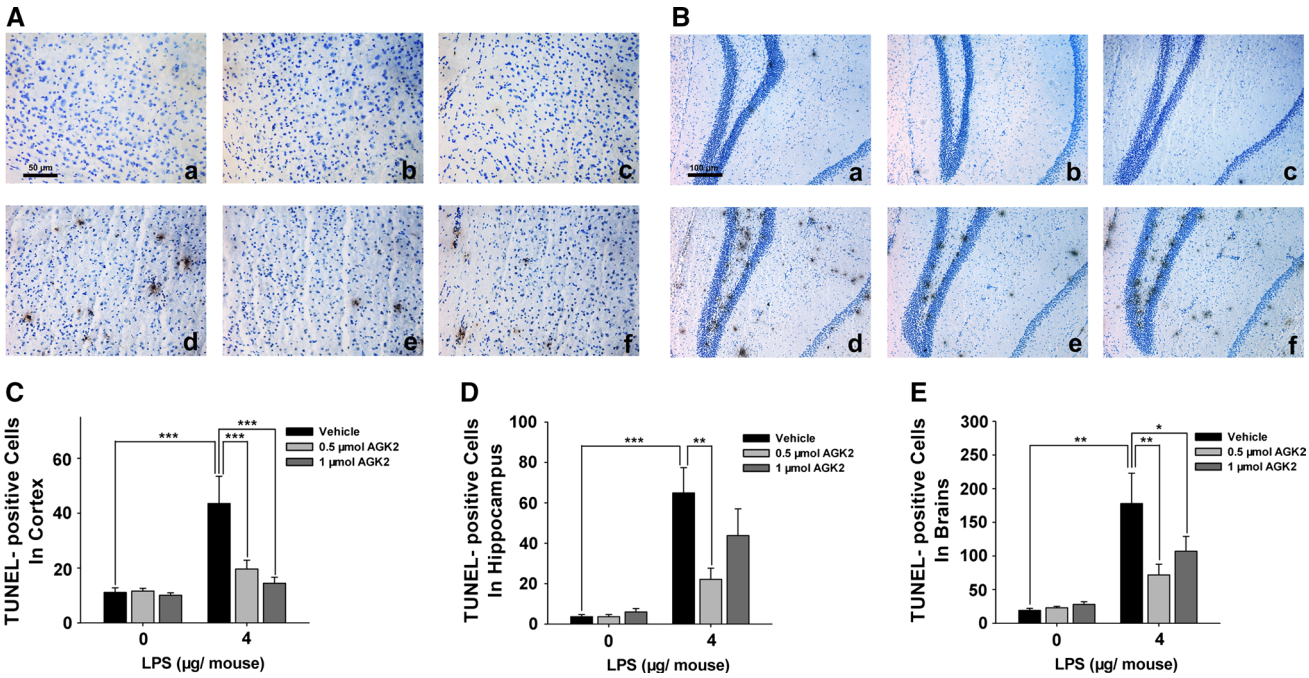

Fig. 4 SIRT2 inhibitor AGK2 significantly decreased the LPS-induced TUNEL signals in mouse brains. Representative TUNEL images in the cortex (**a**) and hippocampus (**b**) of mouse brains 24 h after the drug administration. *a–f* stand for the following groups respectively: vehicle group, n = 15; 0.5 μmol AGK2 group, n = 5; 1 μmol AGK2 group, n = 5; LPS group (4 μg per mouse), n = 20; LPS (4 μg per mouse) and 0.5 μmol AGK2 co-administration group, n = 15; LPS and 1 μmol AGK2 co-administration group, n = 15. Neither in the cortex (**a**) or the hippocampus (**b**), there was significant difference between the vehicle group (*a*) and the AGK2 treatment-only groups (*b*, c). There was a marked increase in the TUNEL-positive signals in the LPS group (*d*), which was blocked by the treatment of both doses of AGK2 (*e*, *f*). **c** Quantifications of TUNEL-positive cells in the cortex. Intraventricularly injected LPS induced a significant increase in the TUNEL-positive cells, which was inhibited by simultaneous administration of AGK2 (0.5 or 1 μmol per mouse). **d** Quantifications of TUNEL-positive cells in the hippocampus. Intraventricularly injected LPS induced a significant increase in the TUNEL-positive cells, which was blocked by simultaneous administration of AGK2 (0.5 μmol per mouse). **e** Quantifications of all the TUNEL-positive cells in mouse brains. AGK2 (0.5 or 1 μmol per mouse) prevented the LPS-induced increase in the TUNEL-positive cells. *Error bars* indicate the standard error of the mean (SEM). *$p < 0.05$; **$p < 0.01$. ***$p < 0.001$ (Color figure online)

in the LPS-induced neuroinflammation in vivo, since AGK2 can markedly decrease LPS-induced increases in the CD11b signals and the mRNA levels of TNF-α and IL-6. Moreover, we found that AGK2 can block the translocation of NFκB stimulated by LPS from the cytosol to the nucleus. Due to the critical roles of nuclear translocation of NFκB in inflammation [42–46], our study has suggested that SIRT2 could mediate neuroinflammation by modulating nuclear translocation of NFκB. These observations, together with our previous finding that SIRT2 silencing can lead to decreased LPS-induced microglial activation—a major event in neuroinflammation [16], have collectively suggested that SIRT2 activity may be required for LPS-induced neuroinflammation. These observations have also suggested that the SIRT2 inhibition-produced decreases in the brain injury in the models of PD, HD and cerebral ischemia may result from the capacity of SIRT2 inhibition to decrease neuroinflammation. Our observations are also consistent with the study showing that SIRT2 deficiency led to decreased LPS-induced inflammation in bone marrow-derived macrophages [47].

There are other studies suggesting that SIRT2 inhibition can enhance inflammatory responses: By applying a low LPS dosage (0.2 μg LPS per mouse), Pais et al. [17] used SIRT2 knockout mice to study the effect of SIRT2 deficiency on microglial activation and the mRNA levels of cytokines, showing that SIRT2 deficiency led to increased LPS-induced neuroinflammation. We propose the following reasons for explaining the seemingly contradicting observations regarding the roles of SIRT2 in neuroinflammation in their study and our studies: Our study applied 4 μg LPS per mouse, which is in the same range of the LPS dosage as widely used in the mouse model of LPS-induced neuroinflammation (2–25 μg LPS per mouse) [25, 48–52]. In contrast, Pais et al. used an exceedingly low dosage of LPS (0.2 μg LPS per mouse), which could activate a dramatically different signaling transduction pathway as that was activated in our current study. In the cellular model of neuroinflammation, our previous study was also significantly different from the study of *Pais* et al.: Our previous study used 500–1000 ng/mL LPS [16], while Pais et al. used TNF-α together with a relatively low concentration of LPS

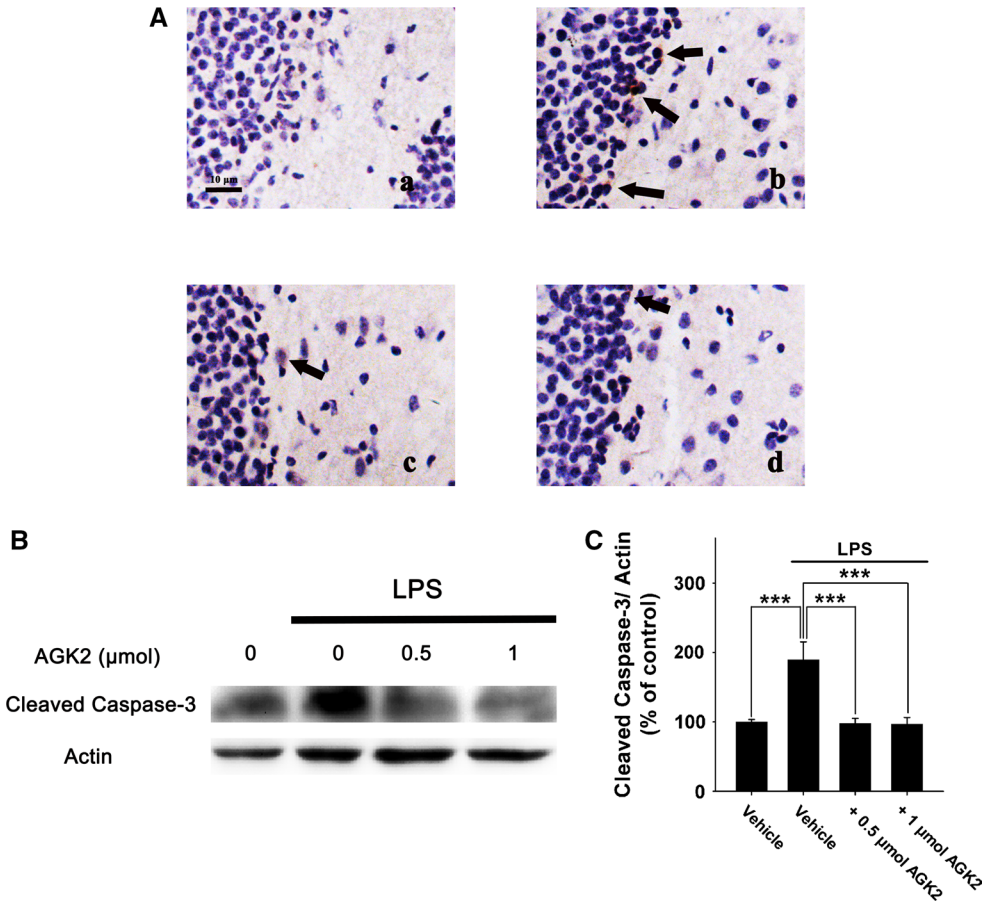

Fig. 5 SIRT2 inhibitor AGK2 blocked the LPS-induced increase in the cleaved Caspase-3 signals in mouse brains. **a** Representative immunohistochemical images of cleaved Caspase-3 in mouse brains 24 h after the drug administration. LPS induced a significant increase in cleaved Caspase-3 signals, which was blocked by simultaneous administration of AGK2. *a–d* stand for the following groups, respectively: Vehicle group; LPS (4 μg per mouse) group; LPS (4 μg per mouse) and 0.5 μmol AGK2 co-administration group; LPS (4 μg per mouse) and 1 μmol AGK2 co-administration group (15–20 mice in each group). **b** Representative Western blot for the cleaved Caspase-3 levels in whole brains. The mice were intraventricularly co-injected with LPS (4 μg per mouse) and AGK2 (0.5 or 1 μmol per mouse) 24 h before protein was extracted. **c** Quantifications of the protein levels of Caspase-3 in mouse brains. Intraventricularly injected LPS led to a significant increase in cleaved Caspase-3, which was blocked by AGK2 (0.5 or 1 μmol per mouse). Six mice in each group. *Error bars* indicate the standard error of the mean (SEM). ***$p < 0.001$ (Color figure online)

(50 ng/mL) to induce inflammation. Multiple studies have suggested that SIRT2 could produce contrasting roles in cell death [53, 54] and oxidative stress [17, 47, 55] under different conditions, suggesting that SIRT2, like calcium, can play complex roles in certain biological processes. We propose that SIRT2 mediates the neuroinflammation induced by relatively high concentrations of LPS, while SIRT2 activity produces an inhibitory effect on the neuroinflammation induced by relatively low concentrations of LPS. Future studies are needed to investigate mechanisms underlying the complex roles of SIRT2 in biological processes, which are of great significance for understand the biological functions of SIRT2.

Our study has shown that AGK2 can decrease not only LPS-induced increase in TUNEL signals—a marker of apoptosis-like damage, but also LPS-induced increases in the levels of active Caspase-3 and Bax. These studies have suggested that SIRT2 also plays a significant role in LPS-induced cellular apoptosis in the brain. Because it is established that LPS-induced neuroinflammation can induce brain damage by generating oxidative stress and cytokines [25, 50–52, 56], it is reasonable to propose that AGK2 decreases LPS-induced brain damage by blocking LPS-induced neuroinflammation.

In summary, our current study has suggested that SIRT2 plays critical roles in LPS-induced neuroinflammation and

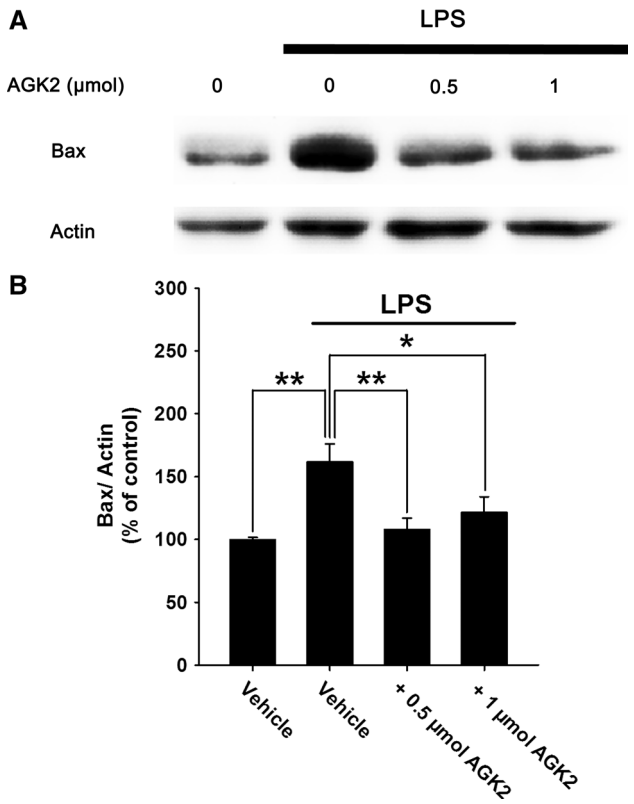

Fig. 6 SIRT2 inhibitor AGK2 prevented the LPS-induced increase in the protein level of Bax in mouse brains. **a** Representative Western blot for the Bax levels in whole brains. The mice were intraventricularly co-injected with LPS (4 μg per mouse) and AGK2 (0.5 or 1 μmol per mouse) 24 h before protein was extracted. **b** Quantifications of the protein levels of Bax in mouse brains. Intraventricularly injected LPS significantly increased the protein level of Bax, which was prevented by AGK2. Six mice in each group *Error bars* indicate the standard error of the mean (SEM). $*p < 0.05$; $**p < 0.01$

brain damage. SIRT2 may become a new therapeutic target for decreasing the neuroinflammation in multiple major neurological diseases.

Acknowledgments This study was supported by Chinese National Natural Science Foundation Grants #81171098 and #81271305 (to W. Y.), and Chinese National Natural Science Foundation Grants #61227071 (to X. W.).

References

1. Guarente L (2000) Sir2 links chromatin silencing, metabolism, and aging. Genes Dev 14:1021–1026
2. Herskovits AZ, Guarente L (2013) Sirtuin deacetylases in neurodegenerative diseases of aging. Cell Res 23:746–758
3. Hall JA, Dominy JE, Lee Y, Puigserver P (2013) The sirtuin family's role in aging and age-associated pathologies. J Clin Invest 123:973–979
4. Mouchiroud L, Houtkooper RH, Moullan N, Katsyuba E, Ryu D, Cantó C, Mottis A, Jo Y-S, Viswanathan M, Schoonjans K (2013) The NAD^+/sirtuin pathway modulates longevity through activation of mitochondrial UPR and FOXO signaling. Cell 154:430–441
5. Nogueiras R, Habegger KM, Chaudhary N, Finan B, Banks AS, Dietrich MO, Horvath TL, Sinclair DA, Pfluger PT, Tschöp MH (2012) Sirtuin 1 and sirtuin 3: physiological modulators of metabolism. Physiol Rev 92:1479–1514
6. Eskandarian HA, Impens F, Nahori M-A, Soubigou G, Coppée J-Y, Cossart P, Hamon MA (2013) A role for SIRT2-dependent histone H3K18 deacetylation in bacterial infection. Science 341:1238858
7. Kanfi Y, Naiman S, Amir G, Peshti V, Zinman G, Nahum L, Bar-Joseph Z, Cohen HY (2012) The sirtuin SIRT6 regulates lifespan in male mice. Nature 483:218–221
8. Donmez G, Outeiro TF (2013) SIRT1 and SIRT2: emerging targets in neurodegeneration. EMBO Mol Med 5:344–352
9. Krey L, Luhder F, Kusch K, Czech-Zechmeister B, Konnecke B, Outeiro TF, Trendelenburg G (2015) Knockout of silent information regulator 2 (SIRT2) preserves neurological function after experimental stroke in mice. J Cereb Blood Flow metab 35:2080–2088
10. Liu L, Arun A, Ellis L, Peritore C, Donmez G (2014) SIRT2 enhances 1-methyl-4-phenyl-1,2,3,6-tetrahydropyridine (MPTP)-induced nigrostriatal damage via apoptotic pathway. Front Aging Neurosci 6:184
11. Outeiro TFKE, Altmann SM, Kufareva I, Strathearn KE, Amore AM, Volk CB, Maxwell MM, Rochet JC, McLean PJ, Young AB, Abagyan R, Feany MB, Hyman BT, Kazantsev AG (2007) Sirtuin 2 inhibitors rescue alpha-synuclein-mediated toxicity in models of Parkinson's disease. Science 317:516–519
12. Chopra V, Quinti L, Kim J, Vollor L, Narayanan KL, Edgerly C, Cipicchio PM, Lauver MA, Choi SH, Silverman RB, Ferrante RJ, Hersch S, Kazantsev AG (2012) The sirtuin 2 inhibitor AK-7 is neuroprotective in Huntington's disease mouse models. Cell Rep 2:1492–1497
13. Zhao J, Mou Y, Bernstock JD, Klimanis D, Wang S, Spatz M, Maric D, Johnson K, Klinman DM, Li X, Li X, Hallenbeck JM (2015) Synthetic oligodeoxynucleotides containing multiple telemeric TTAGGG motifs suppress inflammasome activity in macrophages subjected to oxygen and glucose deprivation and reduce ischemic brain injury in stroke-prone spontaneously hypertensive rats. PLoS One 10:e0140772
14. Frank-Cannon TC, Alto LT, McAlpine FE, Tansey MG (2009) Does neuroinflammation fan the flame in neurodegenerative diseases. Mol Neurodegener 4:1–13
15. Hirsch EC, Hunot S (2009) Neuroinflammation in Parkinson's disease: a target for neuroprotection? Lancet Neurol 8:382–397
16. Chen H, Wu D, Ding X, Ying W (2015) SIRT2 is required for lipopolysaccharide-induced activation of BV2 microglia. NeuroReport 26:88–93
17. Pais TF, Szego EM, Marques O, Miller-Fleming L, Antas P, Guerreiro P, de Oliveira RM, Kasapoglu B, Outeiro TF (2013) The NAD-dependent deacetylase sirtuin 2 is a suppressor of microglial activation and brain inflammation. EMBO J 32:2603–2616
18. Yuan F, Xu ZM, Lu LY, Nie H, Ding J, Ying WH, Tian HL (2016) SIRT2 inhibition exacerbates neuroinflammation and blood-brain barrier disruption in experimental traumatic brain injury by enhancing NF-kappaB p65 acetylation and activation. J Neurochem 136:581–593
19. Hanslick JL, Lau K, Noguchi KK, Olney JW, Zorumski CF, Mennerick S, Farber NB (2009) Dimethyl sulfoxide (DMSO) produces widespread apoptosis in the developing central nervous system. Neurobiol Dis 34:1–10
20. Ma Y, Jiang J, Wang L, Nie H, Xia W, Liu J, Ying W (2012) CD38 is a key enzyme for the survival of mouse microglial BV2 cells. Biochem Biophys Res Commun 418:714–719

21. Wang B, Ma Y, Kong X, Ding X, Gu H, Chu T, Ying W (2014) NAD^+ administration decreases doxorubicin-induced liver damage of mice by enhancing antioxidation capacity and decreasing DNA damage. Chem Biol Interact 212:65–71
22. Ma Y, Cao W, Wang L, Jiang J, Nie H, Wang B, Wei X, Ying W (2014) Basal CD38/cyclic ADP-ribose-dependent signaling mediates ATP release and survival of microglia by modulating connexin 43 hemichannels. Glia 62:943–955
23. Han ZY, Shen FX, He Y, Degos V, Camus M, Maze M, Young WL, Su H (2014) Activation of alpha-7 nicotinic acetylcholine receptor reduces ischemic stroke injury through reduction of pro-inflammatory macrophages and oxidative stress. PLoS One 9:e105711
24. Liu T, Zhang T, Yu H, Shen H, Xia W (2014) Adjudin protects against cerebral ischemia reperfusion injury by inhibition of neuroinflammation and blood-brain barrier disruption. J Neuroinflammation 11:107
25. Tanaka S, Ishii A, Ohtaki H, Shioda S, Yoshida T, Numazawa S (2013) Activation of microglia induces symptoms of Parkinson's disease in wild-type, but not in IL-1 knockout mice. J Neuroinflammation 10:143
26. Kuwabara Y, Yokoyama A, Yang L, Toku K, Mori K, Takeda I, Shigekawa T, Zhang B, Maeda N, Sakanaka M, Tanaka J (2003) Two populations of microglial cells isolated from rat primary mixed glial cultures. J Neurosci Res 73:22–30
27. Hanisch U-K, Kettenmann H (2007) Microglia: active sensor and versatile effector cells in the normal and pathologic brain. Nat Neurosci 10:1387–1394
28. Boche D, Perry V, Nicoll J (2013) Review: activation patterns of microglia and their identification in the human brain. Neuropathol Appl Neurobiol 39:3–18
29. Giridharan VV, Thandavarayan RA, Arumugam S, Mizuno M, Nawa H, Suzuki K, Ko KM, Krishnamurthy P, Watanabe K, Konishi T (2015) Schisandrin B ameliorates ICV-infused amyloid beta induced oxidative stress and neuronal dysfunction through inhibiting RAGE/NF-kappaB/MAPK and up-regulating HSP/Beclin expression. PLoS One 10:e0142483
30. Li W, Chen Z, Yan M, He P, Chen Z, Dai H (2016) The protective role of Isorhamnetin on human brain microvascular endothelial cells from cytotoxicity induced by methylglyoxal and oxygen glucose deprivation. J Neurochem 136:651–659
31. Michelucci A, Bithell A, Burney MJ, Johnston CE, Wong K-Y, Teng S-W, Desai J, Gumbleton N, Anderson G, Stanton LW, WilliamsBP, Buckley NJ (2015) The neurogenic potential of astrocytes is regulated by inflammatory signals. Mol Neurobiol. doi:10.1007/s12035-015-9296-x
32. Buckley SM, Delhove JM, Perocheau DP, Karda R, Rahim AA, Howe SJ, Ward NJ, Birrell MA, Belvisi MG, Arbuthnot P, Johnson MR, Waddington SN, McKay TR (2015) In vivo bioimaging with tissue-specific transcription factor activated luciferase reporters. Sci Rep 5:11842
33. Fernandes A, Miller-Fleming L, Pais TF (2014) Microglia and inflammation: conspiracy, controversy or control? CMLS 71:3969–3985
34. Satoh A, S-i Imai (2014) Systemic regulation of mammalian ageing and longevity by brain sirtuins. Nat Commun 5:4211
35. Maxwell MM, Tomkinson EM, Nobles J, Wizeman JW, Amore AM, Quinti L, Chopra V, Hersch SM, Kazantsev AG (2011) The Sirtuin 2 microtubule deacetylase is an abundant neuronal protein that accumulates in the aging CNS. Hum Mol Genet 20:3986–3996
36. Michan S, Sinclair D (2007) Sirtuins in mammals: insights into their biological function. Biochem J 404:1–13
37. Suzuki K, Koike T (2007) Mammalian Sir2-related protein (SIRT) 2–mediated modulation of resistance to axonal degeneration in slow Wallerian degeneration mice: a crucial role of tubulin deacetylation. Neuroscience 147:599–612
38. Yu TT, McIntyre JC, Bose SC, Hardin D, Owen MC, McClintock TS (2005) Differentially expressed transcripts from phenotypically identified olfactory sensory neurons. J Comp Neurol 483:251–262
39. Werner HB, Kuhlmann K, Shen S, Uecker M, Schardt A, Dimova K, Orfaniotou F, Dhaunchak A, Brinkmann BG, Möbius W (2007) Proteolipid protein is required for transport of sirtuin 2 into CNS myelin. J Neurosci 27:7717–7730
40. Southwood CM, Peppi M, Dryden S, Tainsky MA, Gow A (2007) Microtubule deacetylases, SirT2 and HDAC6, in the nervous system. Neurochem Res 32:187–195
41. Li W, Zhang B, Tang J, Cao Q, Wu Y, Wu C, Guo J, Ling EA, Liang F (2007) Sirtuin 2, a mammalian homolog of yeast silent information regulator-2 longevity regulator, is an oligodendroglial protein that decelerates cell differentiation through deacetylating alpha-tubulin. J Neurosci 27:2606–2616
42. Xiao C, Ghosh S (2005) NF-kappaB, an evolutionarily conserved mediator of immune and inflammatory responses. Adv Exp Med Biol 560:41–45
43. Trapecar M, Goropevsek A, Gorenjak M, Gradisnik L, Rupnik MS (2014) A co-culture model of the developing small intestine offers new insight in the early immunomodulation of enterocytes and macrophages by Lactobacillus spp. through STAT1 and NF-kB p65 translocation. PLoS One 9:e86297
44. Sangiovanni E, Vrhovsek U, Rossoni G, Colombo E, Brunelli C, Brembati L, Trivulzio S, Gasperotti M, Mattivi F, Bosisio E (2013) Ellagitannins from Rubus berries for the control of gastric inflammation: in vitro and in vivo studies. PLoS One 8:e71762
45. Farruggia C, Yang Y, Kim B, Pham T, Bae M, Park Y-K, Lee J-Y (2015) Astaxanthin plays anti-inflammatory and antioxidant effects by inhibiting NFkB nuclear translocation and NOX2 expression in macrophages. FASEB J 29(603):608
46. Shao J, Liu T, Xie QR, Zhang T, Yu H, Wang B, Ying W, Mruk DD, Silvestrini B, Cheng CY, Xia W (2013) Adjudin attenuates lipopolysaccharide (LPS)- and ischemia-induced microglial activation. J Neuroimmunol 254:83–90
47. Lee AS, Jung YJ, Kim D, Nguyen-Thanh T, Kang KP, Lee S, Park SK, Kim W (2014) SIRT2 ameliorates lipopolysaccharide-induced inflammation in macrophages. Biochem Biophys Res Commun 450:1363–1369
48. Lo U, Selvaraj V, Plane J, Chechneva O, Otsu K, Deng W (2014) p38α (MAPK14) critically regulates the immunological response and the production of specific cytokines and chemokines in astrocytes. Sci Rep 4:7405
49. Gao HM, Kotzbauer PT, Uryu K, Leight S, Trojanowski JQ, Lee VMY (2008) Neuroinflammation and oxidation/nitration of alpha-synuclein linked to dopaminergic neurodegeneration. J Neurosci 28:7687–7698
50. Murray CL, Skelly DT, Cunningham C (2011) Exacerbation of CNS inflammation and neurodegeneration by systemic LPS treatment is independent of circulating IL-1beta and IL-6. J Neuroinflammation 8:50
51. Xiang Y, Chen L, Liu H, Liu X, Wei X, Sun B, Wang T, Zhang X (2013) Inhibition of sPLA (2)-IIA prevents LPS-induced neuroinflammation by suppressing ERK1/2-cPLA (2) alpha pathway in mice cerebral cortex. PLoS One 8:e77909
52. Grin'kina NM, Karnabi EE, Damania D, Wadgaonkar S, Muslimov IA, Wadgaonkar R (2012) Sphingosine kinase 1 deficiency exacerbates LPS-induced neuroinflammation. PLoS One 7:e36475
53. Li Y, Matsumori H, Nakayama Y, Osaki M, Kojima H, Kurimasa A, Ito H, Mori S, Katoh M, Oshimura M, Inoue T (2011) SIRT2 down-regulation in HeLa can induce p53 accumulation via p38

MAPK activation-dependent p300 decrease, eventually leading to apoptosis. Genes Cells 16:34–45
54. He X, Nie H, Hong Y, Sheng C, Xia W, Ying W (2012) SIRT2 activity is required for the survival of C6 glioma cells. Biochem Biophys Res Commun 417:468–472
55. Lynn EG, McLeod CJ, Gordon JP, Bao JJ, Sack MN (2008) SIRT2 is a negative regulator of anoxia-reoxygenation tolerance via regulation of 14-3-3 zeta and BAD in H9c2 cells. FEBS Lett 582:2857–2862
56. Kurauchi Y, Hisatsune A, Isohama Y, Mishima S, Katsuki H (2012) Caffeic acid phenethyl ester protects nigral dopaminergic neurons via dual mechanisms involving haem oxygenase-1 and brain-derived neurotrophic factor. Br J Pharmacol 166:1151–1168